Lawrence Berkeley National Laboratory
Recent Work

Title
Spin-orbit torque and Nernst effect in Bi-Sb/Co heterostructures

Authors
Roschewsky, N
Walker, ES
Gowtham, P
et al.

Spin-Orbit Torque and Nernst Effect in BiSb/Co Heterostructures

Niklas Roschewsky,[1, *] Emily S. Walker,[2] Praveen Gowtham,[3]
Frances Hellman,[1, 4] Seth R. Bank,[2] and Sayeef Salahuddin[3, 4, †]

[1] Department of Physics, University of California, Berkeley, California 94720, USA
[2] Microelectronics Research Center and Department of Electrical and
Computer Engineering, University of Texas, Austin, Texas 78758, USA
[3] Department of Electrical Engineering and Computer Sciences, University of California, Berkeley, California 94720, USA
[4] Materials Science Division, Lawrence Berkeley National Laboratory, Berkeley, California 94720, USA
(Dated: October 1, 2018)

Harmonic measurements of the longitudinal and transverse voltages in BiSb/Co bilayers are presented. A large second harmonic voltage signal due to the ordinary Nernst effect is observed. In experiments where a magnetic field is rotated in the film plane, the ordinary Nernst effect shows the same angular dependence in the transverse voltage as the damping-like spin-orbit torque and in the longitudinal voltage as the unidirectional spin-Hall magneto-resistance respectively. Therefore, the ordinary Nernst effect can be a spurious signal in spin-orbit torque measurements, leading to an overestimation of the spin-Hall angle in topological insulators.

In metal-based spintronics, heavy metals such as platinum, tantalum or tungsten are used to convert charge currents into spin-currents via the spin-Hall or Rashba-Edelstein effect [1–4]. These spin currents can be used to manipulate the magnetization of a magnet, which has useful application in memory technology [5, 6].

One way to quantify the spin-to-charge conversion efficiency is to measure the the spin-Hall angle θ_{SH}. While the reported magnitude of the spin-Hall angle fluctuates somewhat in the literature, it is generally agreed upon that the spin-Hall angle in heavy metals is of the order of 10% [7]. To make a significant impact in the memory applications, a larger spin-to-charge conversion efficiency, i.e., a larger spin Hall angle is desired [8, 9]. In this regard, topological insulators gained immense interest recently due to the unique spin-momentum locking they offer, which could lead to significantly higher spin to charge conversion efficiency. Indeed, various research groups have reported the observation of large spin Hall angles compared to those observed in heavy metal layers using various characterization methods, such as harmonic Hall voltage measurements [10, 11], spin pumping [12–16], spin-Seebeck effect measurements [17], spin-polarized tunneling studies [18, 19], domain wall motion experiments [20, 21] and spin-torque ferromagnetic resonance [22–26].

In addition, it has been reported that the unidirectional spin-Hall magneto-resistance (USMR) is orders of magnitudes larger in topological insulator/ heavy metal bilayers films than in conventional heavy metal/ ferromagnet bilayers [27–30]. Since the unidirectional magneto-resistance is asymmetric in the current direction as well as the magnetic field direction, harmonic voltage measurements are often used to quantify this phenomenon [31].

While these aforementioned reports have given credence to the promise of using topological insulator materials for high efficiency electronics applications, there are also some recent reports that indicate how the extracted spin Hall angles could be impacted by spurious signals. For example, Yasuda *et al.* [32] have discussed how asymmetric magnon scattering could influence the magnitude of the spin Hall angle. Similarly, it has been observed recently that the Seebeck effect can be a spurious signal in spin-pumping experiments [33]. From both the points of view of understanding the underlying physics and its ultimate adoption for an application, it is important to identify the sources of spurious signals in the quantification of the spin Hall angle. In this work, we show that there is an additional source, stemming from the ordinary
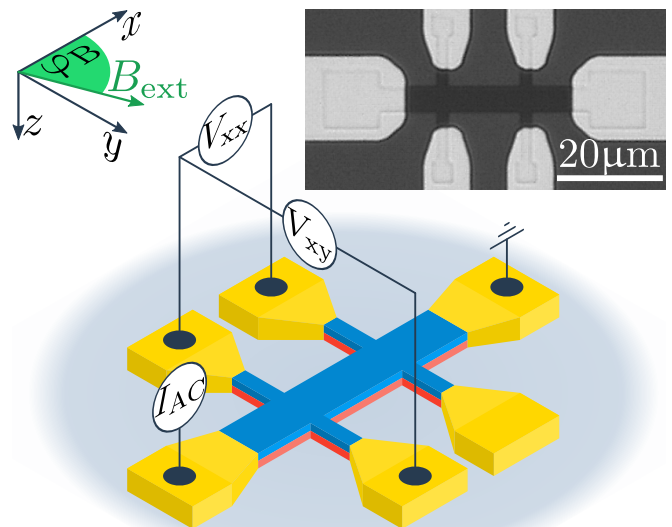

FIG. 1. A double Hall-bar structure is used to measure transverse (V_{xy}) and longitudinal (V_{xx}) voltages on the BiSb bilayer samples considered in this work. The magnetic field is applied in the film plane at an angle φ with respect to the current direction. The inset shows a micro-graph of an actual double Hall-bar device. The with of the Hall-bar is 6 µm.

Nernst effect (ONE) [34, 35], that could significantly influence the observations made in harmonic Hall measurements, especially for semiconducting spin Hall materials such as the topological insulators.

Notably, ONE refers to the generation of a voltage, when both a temperature gradient and a magnetic field are present [36]. The thermal voltage scales linearly with the external magnetic field and has not been taken into account in previous SOT experiments. Therefore the presence of the ONE in topological insulators at room temperature might give an explanation for the giant spin Hall angle reported recently. Further the ONE can contribute to the longitudinal voltage signal in USMR-type measurements.

Two control experiments will be discussed in the following to separate thermal effects from SOT and USMR. First, we will compare the harmonic voltage response in BiSb/Co samples to that in BiSb/Al samples. While in BiSb/Co, voltages can arise due to magneto-transport effects, the effects in BiSb/Al will be purely thermomagnetic. Secondly we will explore the magnetic field dependence of the voltage response. While spin-transport effects are expected to be suppressed by large magnetic fields, the thermal voltage due to the ONE scales linearly with magnetic field.

The samples discussed in this work are $Bi_{0.74}Sb_{0.26}(4)/Co(4)$, $Bi_{0.96}Sb_{0.04}(10)/Al(5)$ and $Pt(5)/Py(5)$ (thickness in nm). We refer to these samples as BiSb/Co, BiSb/Al and Pt/Py respectively. All samples are capped with 2.5 nm Si_3N_4. The BiSb is grown epitaxially on high resistivity Si(111) substrate by molecular beam epitaxy. Bulk samples of both $Bi_{0.74}Sb_{0.26}$ and $Bi_{0.96}Sb_{0.04}$ are semi-metals [37, 38]. It has been reported that a band gap opens up in thin films of $Bi_{0.74}Sb_{0.26}$ due to quantum confinement effects. Therefore $Bi_{0.74}Sb_{0.26}$ films may show topological insulating behavior [39].

Co is deposited with e-beam evaporation onto the BiSb ex-situ and has in-plane magnetic anisotropy. Al, Pt and Py are grown by magnetron sputtering. After growth, optical lithography and Ar-ion milling are used to pattern Hall bar devices, as shown in the inset of Fig. 1. The width of the Hall bar is 6 μm and the distance between 2 Hall crosses is 20 μm. The current is applied along the x-direction while the longitudinal and transverse voltages (V_{xx} and V_{xy}) are measured. An external magnetic field B_{ext} is applied in the film plane at an angle φ_B with respect to the current direction.

In all experiments reported here the magnetic field is sufficient to fully saturate the magnet along the field-direction. Further, all experiments were performed at room temperature and at constant Joule-heating power of $P_{heat} = I^2R = 0.18\,mW$.

For harmonic measurements presented in this work, an ac current $I = I_0 \cdot \sin(\omega t)$ with $\omega/2\pi = 1.5\,kHz$ is applied. If SOT is present, the ac current can induce quasi static magnetization oscillations and thus periodic changes of the resistance and Hall resistance. Therefore, in addition to the first harmonic voltage response V^ω, a second harmonic voltage $V^{2\omega}$ will be induced at twice the excitation frequency [40].

Further, the ac current induces a periodic temperature gradient. Since Joule heating is quadratic in the current, a second harmonic voltage response can also be induced by thermal effects such as the ordinary Nernst effect [34, 41], the anomalous Nernst effect [40, 42] or the longitudinal spin-Seebeck effect [43].

The first harmonic Hall voltage can be written as:

$$V_{1\omega}^{xy} = V_{PHE} \cdot \sin(2\varphi_B),$$
$$V_{1\omega}^{xx} = V_{AMR} \cdot \cos(2\varphi_B).$$

Here, φ_B is the angle between the current and the external magnetic field B_{ext} in the film plane (cf. Fig. 1), V_{PHE} is the planar Hall effect amplitude and V_{AMR} is the amplitude of the anisotropic magneto-resistance. The second harmonic voltage is written as [40]:

$$V_{xy}^{2\omega} = \left(\frac{V_{AHE}}{2}\frac{\Delta B_{DL}}{B_{ext} + \mu_0 M_{eff}} + A\alpha\nabla T + N\alpha B_{ext}\nabla T\right)\cos(\varphi_B) + \left(V_{PHE}\frac{\Delta B_{FL}}{B_{ext}}\right)\cos(2\varphi_B)\cos(\varphi_B), \quad (1)$$

$$V_{xx}^{2\omega} = \left(V_{USMR} + A\beta\nabla T + N\beta B_{ext}\nabla T\right)\sin(\varphi_B) + \left(V_{AMR}\frac{\Delta B_{FL}}{B_{ext}}\right)\sin(2\varphi_B)\cos(\varphi_B). \quad (2)$$

V_{AHE} is the anomalous Hall effect voltage, ΔB_{DL} is the effective field due to the damping like torque, $\mu_0 M_{eff}$ is the effective magnetization, A is the coefficient for the ANE and SSE, α and β are geometrical factors, ΔT is the temperature gradient, N is the ordinary Nernst coefficient, ΔB_{DL} is the effective field due to field-like torque and V_{USMR} is the amplitude of the unidirectional spin-Hall magneto-resistance.

The field-like SOT can be extracted from the φ_B dependence of the second Harmonic voltage signal. However, it is important to consider the magnetic field dependence in addition to the φ_B-dependence for the ex-
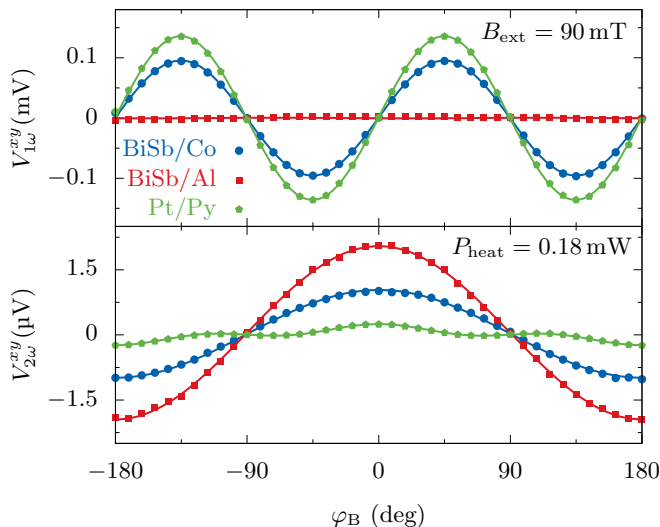
FIG. 2. Upper panel: The planar Hall effect is only observed in the samples with magnetic layers (BiSb/Co and Pt/Py). Here, φ_B is the angle between the current direction and B_{ext} in the film plane. Lower panel: $V_{2\omega}$ shows a $\cos(\varphi_B)$ dependence in the samples with BiSb, due to the ordinary Nernst effect. In the sample Pt/Py, spin-orbit torque and anomalous Nernst effect are present. The solid lines are fits to eq.(1).

FIG. 3. Upper panel: $V_{1\omega}^{xx}$ as a function of φ_B. A constant offset was removed for easy comparison. The anisotropic magneto-resistance is observed only in the magnetic samples, BiSb/Co and Pt/Py. Lower panel: $V_{2\omega}^{xx}$ in BiSb/Co and BiSb/Al shows a $\sin(\varphi)$ dependence. This is expected from the ordinary Nernst effect. In the sample Pt/Py contributions from spin-orbit torque, anomalous Nernst effect and the unidirectional spin-Hall magneto-resistance are observed. The solid lines are fits to Eq.(2).

traction of the damping-like SOT, as well as the USMR, to distinguish magneto-thermal effects from SOT.

We start by discussing the angular dependence of the transverse harmonic voltages. The top panel in Fig. 2 shows $V_{xy}^{1\omega}$ as a function of φ_B. In the samples BiSb/Co and Pt/Py, a $\sin(2\varphi_B)$-dependence can be seen. This is due to the presence of the PHE in the Co and Py layers respectively. $V_{xy}^{1\omega}$ does not depend on B_{ext} in BiSb/Al, due to the absence of a magnetic layer.

The second harmonic Hall voltage $V_{xy}^{2\omega}$ is shown in the bottom panel of Fig. 2. In all 3 samples under consideration, $V_{xy}^{2\omega}$ vs. φ_B can be well fitted by Eq. (1) (solid lines). In the Pt/Py sample contributions from the field-like torque are clearly visible. On the other hand, samples BiSb/Co and BiSb/Al do not show the characteristic $\cos(2\varphi_B)\cos(\varphi_B)$-dependence. Since no magnet is present in the sample BiSb/Al, the large second harmonic voltage is attributed to the ONE.

The fact that no field-like torque is observed in the sample BiSb/Co, as well as the fact that voltage signals in BiSb/Al and BiSb/Co are comparable gives rise to the suspicion that the signal in the sample BiSb/Co might be dominated by the ONE. To unambiguously distinguish the ONE from SOT, the B_{ext}-dependence will have to be considered, which we have discussed after the following discussion on USMR measurements.

In addition to the angular dependence of V_{xy}, the longitudinal voltage V_{xx} was measured (Fig. 3). Again, a signal from the anisotropic magneto-resistance (AMR) is
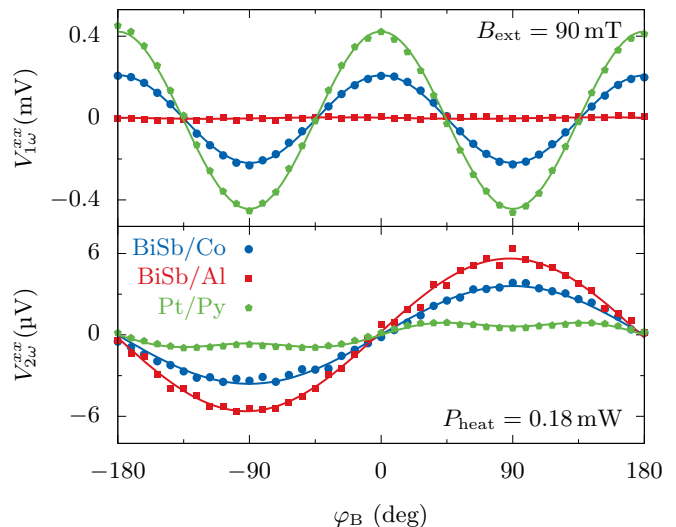
only observed in the samples with magnetic layer (top panel), while all samples show an angular dependence of $V_{2\omega}^{xx}$, that can be well described with Eq. (2) (bottom panel). In the Pt/Py reference sample, a clear signature from field-like SOT can be observed while the USMR is small. The sample BiSb/Al shows a $\sin(\varphi)$-dependence due to the ONE. The absence of field-like torque in BiSb/Co, as well as a signal amplitude comparable to the signal in BiSb/Al raises the suspicion that the signal in BiSb/Co is dominated by the ONE and not a large USMR.

To determine the origin of the large voltages observed in BiSb/Co, we repeat the measurements shown in Fig. 2 and Fig. 3 for different values of B_{ext}. Figure 4 shows the $\cos(\varphi_B)$ contribution to $V_{2\omega}^{xy}$ and the $\sin(\varphi_B)$ contribution to $V_{2\omega}^{xx}$ respectively. In the reference sample Pt/Py, $V_{2\omega}^{xy}$ decreases with increasing B_{ext}. This is expected, because large magnetic fields suppress the quasi-static magnetization oscillations induced by SOT (cf. Eq. (1)). On the other hand, $V_{2\omega}^{xy}$ increases linearly with B_{ext} in the samples BiSb/Co and BiSb/Al. This is clear evidence for the presence of ONE. Note that $V_{2\omega}^{xy}$ is ≈ 50 times larger in the samples with BiSb.

Similarly, a clear presence for the USMR is seen only in the sample Pt/Py (Fig. 4, bottom panel): $V_{2\omega}^{xx}$ decreases with increasing B_{ext}, in accordance with recent reports by Avci *et al.* [44] The samples BiSb/Al and BiSb/Co show a linear dependence on B_{ext}, as expected
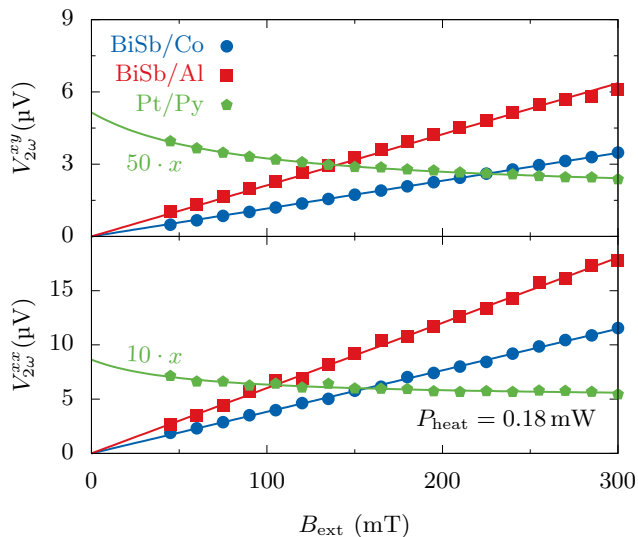
FIG. 4. The magnetic field dependence of the second harmonic voltage. In BiSb/Co and BiSb/Al a linear increase in voltage can be observed, as expected from the ordinary Nernst effect. In Pt/Py on the other hand the harmonic voltage is decreasing as expected from damping-like spin-orbit torque and unidirectional spin-Hall magneto-resistance respectively. Note that the voltage in Pt/Py has been enhances for visual clarity.

from the ONE. The slope of $V_{2\omega}^{xx}$ vs B_{ext} in BiSb/Co is $V_{2\omega}^{xy}/B_{\text{ext}} = (0.011 \pm 0.006)\,\text{V}\,\text{mT}^{-1}$ and $V_{2\omega}^{xx}/B_{\text{ext}} = (0.038 \pm 0.003)\,\text{V}\,\text{mT}^{-1}$ respectively. The different values obtained for the longitudinal and transverse voltages are explained by the geometric factors α and β in eq. 1 and Eq. 2. The ratio is $V_{2\omega}^{xx}/V_{2\omega}^{xy} = \beta/\alpha = l/w = 3.3$, where l is the distance between two Hall crosses and w the width of the Hall bar. This geometrical scaling is a strong indicator that $V_{2\omega}^{xy}$ and $V_{2\omega}^{xx}$ have the same physical origin. Note that USMR and SOT are distinctly different phenomena and it can not be expected that they would scale with the device geometry.

Next we will calculate the ONE coefficient N and show that N is equal in samples BiSb/Co and BiSb/Al. To this end we estimate the temperature gradient using the 1D heat equation $T''(z) = \dot{q}_i/\kappa$, where $T(z)$ is the temperature, $\dot{q}_i$ is the volumetric power density and κ the thermal conductivity. The boundary conditions at the interfaces are:

$$T_i = T_{i+1}\,, \quad \kappa_i \frac{\partial T_i}{\partial z} = \kappa_{i+1}\frac{\partial T_{i+1}}{\partial z}$$

Further, we assume no heat conduction at the top surface and a fixed temperature at the backside of the substrate. The following values for the thermal conductivity have been used: $\kappa_{\text{BiSb}} = 6.8\,\text{W}\,\text{m}^{-1}\,\text{K}^{-1}$ [45], $\kappa_{\text{Co}} = 98\,\text{W}\,\text{m}^{-1}\,\text{K}^{-1}$ [46] and $\kappa_{\text{Al}} = 238\,\text{W}\,\text{m}^{-1}\,\text{K}^{-1}$ [47]. At a heating power of $P = 180\,\mu\text{W}$, the temperature gradient is $\Delta T_{\text{BiSb/Co}} = 6.6\,\text{mK}$ and $\Delta T_{\text{BiSb/Al}} = 18\,\text{mK}$.

Using these values, we find $N = 3 \times 10^{-6}\,\text{V}\,\text{T}^{-1}\,\text{K}^{-1}$ in BiSb/Co and $N = 2.6 \times 10^{-6}\,\text{V}\,\text{T}^{-1}\,\text{K}^{-1}$ in BiSb/Al. These values are well in agreement and confirm the same origin of $V_{2\omega}$ in the samples BiSb/Co and BiSb/Al, namely the ordinary Nernst effect. Further, N is of the same order of magnitude in other semi-conducting materials [48].

In summary, harmonic measurements of the longitudinal and transverse voltages in BiSb/Co films are presented. We find strong evidence that the second harmonic voltage in our samples is dominated by contributions from the ordinary Nernst effect: The longitudinal and transverse voltages are scaling with the device geometry. Further, we show that the ordinary Nernst effect has the same amplitude in BiSb/Al samples, where magneto-transport effects are absent. In fact, we find that the voltages from the ordinary Nernst effect is an order of magnitude larger than voltages expected from SOT or USMR, which makes the detection of pure spin related effects highly challenging. We believe that the semiconducting and therefore highly resistive nature of BiSb is predominantly responsible for the large ONE related voltages observed in our experiments. Given that the symmetry of the ONE related voltages are the same as those originating from spin orbit torque, it is critical to measure to harmonic voltages as a function of the external magnetic field amplitude to distinguish different contributions such as ANE, ONE and SOT/USMR.

* roschewsky@berkeley.edu
† sayeef@berkeley.edu

[1] I. M. Miron, K. Garello, G. Gaudin, P.-J. Zermatten, M. V. Costache, S. Auffret, S. Bandiera, B. Rodmacq, A. Schuhl, and P. Gambardella, Nature **476**, 189 (2011).
[2] K. Garello, I. M. Miron, C. O. Avci, F. Freimuth, Y. Mokrousov, S. Blugel, S. Auffret, O. Boulle, G. Gaudin, and P. Gambardella, Nat Nano **8**, 587 (2013).
[3] L. Liu, C.-F. Pai, Y. Li, H. W. Tseng, D. C. Ralph, and R. A. Buhrman, Science **336**, 555 (2012).
[4] L. Liu, O. J. Lee, T. J. Gudmundsen, D. C. Ralph, and R. A. Buhrman, Phys. Rev. Lett. **109**, 96602 (2012).
[5] S. W. Lee and K. J. Lee, Proceedings of the IEEE **104**, 1831 (2016).
[6] M. Cubukcu, O. Boulle, N. Mikuszeit, C. Hamelin, T. Bracher, N. Lamard, M.-C. Cyrille, L. Buda-Prejbeanu, K. Garello, I. M. Miron, O. Klein, G. de Loubens, V. V. Naletov, J. Langer, B. Ocker,

P. Gambardella, and G. Gaudin, IEEE Transactions on Magnetics **54**, 1 (2018).

[7] J.-C. Rojas-Sánchez, N. Reyren, P. Laczkowski, W. Savero, J.-P. Attané, C. Deranlot, M. Jamet, J.-M. George, L. Vila, and H. Jaffrès, Physical Review Letters **112**, 106602 (2014).

[8] D. Apalkov, B. Dieny, and J. M. Slaughter, Proceedings of the IEEE **104**, 1796 (2016).

[9] Z. Diao, D. Apalkov, M. Pakala, Y. Ding, A. Panchula, and Y. Huai, Applied Physics Letters **87**, 232502 (2005).

[10] Y. Fan, P. Upadhyaya, X. Kou, M. Lang, S. Takei, Z. Wang, J. Tang, L. He, L.-T. Chang, M. Montazeri, G. Yu, W. Jiang, T. Nie, R. N. Schwartz, Y. Tserkovnyak, and K. L. Wang, Nature Materials **13**, 699 (2014).

[11] M. DC, R. Grassi, J.-Y. Chen, M. Jamali, D. Reifsnyder Hickey, D. Zhang, Z. Zhao, H. Li, P. Quarterman, Y. Lv, M. Li, A. Manchon, K. A. Mkhoyan, T. Low, and J.-P. Wang, Nature Materials **17**, 800 (2018).

[12] P. Deorani, J. Son, K. Banerjee, N. Koirala, M. Brahlek, S. Oh, and H. Yang, Physical Review B **90**, 094403 (2014).

[13] Y. Shiomi, K. Nomura, Y. Kajiwara, K. Eto, M. Novak, K. Segawa, Y. Ando, and E. Saitoh, Physical Review Letters **113**, 196601 (2014).

[14] M. Jamali, J. S. Lee, J. S. Jeong, F. Mahfouzi, Y. Lv, Z. Zhao, B. K. Nikolić, K. A. Mkhoyan, N. Samarth, and J.-P. Wang, Nano Letters **15**, 7126 (2015).

[15] H. Wang, J. Kally, J. S. Lee, T. Liu, H. Chang, D. R. Hickey, K. A. Mkhoyan, M. Wu, A. Richardella, and N. Samarth, Physical Review Letters **117**, 076601 (2016).

[16] S. Gupta, S. Kanai, F. Matsukura, and H. Ohno, Japanese Journal of Applied Physics **57**, 020302 (2018).

[17] J. B. S. Mendes, O. Alves Santos, J. Holanda, R. P. Loreto, C. I. L. de Araujo, C.-Z. Chang, J. S. Moodera, A. Azevedo, and S. M. Rezende, Physical Review B **96**, 180415 (2017).

[18] L. Liu, A. Richardella, I. Garate, Y. Zhu, N. Samarth, and C.-T. Chen, Physical Review B **91**, 235437 (2015).

[19] J. S. Lee, A. Richardella, D. R. Hickey, K. A. Mkhoyan, and N. Samarth, Physical Review B **92**, 155312 (2015).

[20] N. H. D. Khang, Y. Ueda, and P. N. Hai, Nature Materials , 808813 (2018).

[21] J. Han, A. Richardella, S. A. Siddiqui, J. Finley, N. Samarth, and L. Liu, Physical Review Letters **119**, 077702 (2017).

[22] Y. Wang, P. Deorani, K. Banerjee, N. Koirala, M. Brahlek, S. Oh, and H. Yang, Physical Review Letters **114**, 257202 (2015).

[23] S. Shi, A. Wang, Y. Wang, R. Ramaswamy, L. Shen, J. Moon, D. Zhu, J. Yu, S. Oh, Y. Feng, and H. Yang, Physical Review B **97**, 041115 (2018).

[24] K. Kondou, R. Yoshimi, A. Tsukazaki, Y. Fukuma, J. Matsuno, K. S. Takahashi, M. Kawasaki, Y. Tokura, and Y. Otani, Nature Physics **12**, 1027 (2016).

[25] Y. Wang, D. Zhu, Y. Wu, Y. Yang, J. Yu, R. Ramaswamy, R. Mishra, S. Shi, M. Elyasi, K.-L. Teo,

Y. Wu, and H. Yang, Nature Communications **8**, 1364 (2017).

[26] A. R. Mellnik, J. S. Lee, A. Richardella, J. L. Grab, P. J. Mintun, M. H. Fischer, A. Vaezi, A. Manchon, E.-A. Kim, N. Samarth, and D. C. Ralph, Nature **511**, 449 (2014).

[27] K. Yasuda, A. Tsukazaki, R. Yoshimi, K. S. Takahashi, M. Kawasaki, and Y. Tokura, Physical Review Letters **117**, 127202 (2016).

[28] T. Ideue, K. Hamamoto, S. Koshikawa, M. Ezawa, S. Shimizu, Y. Kaneko, Y. Tokura, N. Nagaosa, and Y. Iwasa, Nature Physics **13**, 578 (2017).

[29] Y. Lv, J. Kally, D. Zhang, J. S. Lee, M. Jamali, N. Samarth, and J.-P. Wang, Nature Communications **9**, 111 (2018).

[30] P. He, S. S.-L. Zhang, D. Zhu, Y. Liu, Y. Wang, J. Yu, G. Vignale, and H. Yang, Nature Physics (2018), 10.1038/s41567-017-0039-y.

[31] C. O. Avci, K. Garello, A. Ghosh, M. Gabureac, S. F. Alvarado, and P. Gambardella, Nat Phys **11**, 570 (2015).

[32] K. Yasuda, A. Tsukazaki, R. Yoshimi, K. Kondou, K. S. Takahashi, Y. Otani, M. Kawasaki, and Y. Tokura, Physical Review Letters **119**, 137204 (2017).

[33] P. Wang, L. F. Zhou, S. W. Jiang, Z. Z. Luan, D. J. Shu, H. F. Ding, and D. Wu, Physical Review Letters **120**, 047201 (2018).

[34] S. S. Li and T. Rabson, Solid-State Electronics **13**, 153 (1970).

[35] D. Yue, W. Lin, J. Li, X. Jin, and C. L. Chien, Physical Review Letters **121**, 037201 (2018).

[36] T. Aono, Japanese Journal of Applied Physics **9**, 761 (1970).

[37] B. Lenoir, M. Cassart, J.-P. Michenaud, H. Scherrer, and S. Scherrer, Journal of Physics and Chemistry of Solids **57**, 89 (1996).

[38] A. L. Jain, Physical Review **114**, 1518 (1959).

[39] Y. Ueda, N. H. Duy Khang, K. Yao, and P. N. Hai, Applied Physics Letters **110**, 062401 (2017).

[40] C. O. Avci, K. Garello, M. Gabureac, A. Ghosh, A. Fuhrer, S. F. Alvarado, and P. Gambardella, Physical Review B **90**, 224427 (2014).

[41] H. B. Callen, Physical Review **73**, 1349 (1948).

[42] T. C. Chuang, P. L. Su, P. H. Wu, and S. Y. Huang, Physical Review B **96**, 174406 (2017).

[43] M. Schreier, N. Roschewsky, E. Dobler, S. Meyer, H. Huebl, R. Gross, and S. T. B. Goennenwein, Applied Physics Letters **103**, 242404 (2013).

[44] C. O. Avci, J. Mendil, G. S. D. Beach, and P. Gambardella, arXiv (2018), arXiv:1806.05305.

[45] T. Yazaki, Journal of the Physical Society of Japan **25**, 1054 (1968).

[46] Y. Terada, K. Ohkubo, T. Mohri, and T. Suzuki, Metallurgical and Materials Transactions A **34**, 2026 (2003).

[47] O. Paul and H. Baltes, Journal of Micromechanics and Microengineering **3**, 110 (1993).

[48] K. Behnia, M.-A. Méasson, and Y. Kopelevich, Physical Review Letters **98**, 076603 (2007).